Ann. For. Res. 66(1): 3024-3036, 2023
ISSN: 18448135, 20652445

ANNALS OF FOREST RESEARCH
www.e-afr.org

ELECTROSPINNING: OPTIMAL PARAMETERS FOR THE PRODUCTION OF POLYVINYL ALCOHOL NANOFIBERS

Andriws Montoya[1*], José Castillo[1] ando William Andrés Castro López.[2]

1. Laboratorio de Física de Materiales Inorgánicos y Orgánicos, Facultad de Ciencias Básicas, Universidad del Quindío, Armenia 63004, Colombia.
2. Facultad de Ciencias Matemáticas y Naturales. Universidad Distrital Francisco José de Caldas. Bogotá D.C. , Colombia

*admontoyac@uqvirtual.edu.co
jhcastillo@uniquindio.edu.co
wacastrol@udistrital.edu.co

ABSTRACT

Polyvinyl alcohol (PVAL) nanofibers were successfully prepared by electrospinning technique. The analysis performed by Scanning Electron Microscopy (SEM) shows that when the needle-collector distance increases, the average diameters of the fibers obtained decrease. It is also observed that as the concentration of the polymer solution increases, the average fibers' diameter increases, and there is a reduction in the generation of bead-shaped defects. An applied voltage of 19 kV, a needle-collector distance of 11 cm, an injection rate of 1 µL / h, relative humidity of 30%, a temperature of 30 ºC, atmospheric pressure and a solution of 6.66% (*w/V*) are established as optimal parameters for obtaining nanofibers of homogeneous diameter and free of defects. The Fourier transform infrared (FTIR) spectra obtained for the membrane produced by electrospun nanofibers show the same functional groups present in a solid PVAL membrane without electrospinning; however, their transmittance peaks are more intense.

KEYWORDS: Electrospinning, nanofiber, optimal parameters, functional fibers, polymer matrix.

1. INTRODUCTION

For applications in biomedical and pharmaceutical sciences, a synthetic, non-toxic and biodegradable polymer is used [1]; one of them is Polyvinyl alcohol (PVAL), a water-soluble polymer produced industrially by the hydrolysis of polyvinyl acetate, which allows it to be marketed, depending on its degree of hydrolysis, in the high, medium or partially hydrolyzed form [2]; its general chemical formula is $C_2 H_4 O$. It is an excellent film former, emulsifier, viscosity modifier and adhesive, its use has been focused towards biomedical applications, such as hydrogels, including contact lenses, artificial organs and drug delivery systems [3].

In the process of obtaining fibers with good conditions in their morphology, diameter and length, some properties of the polymer must be taken into account, such as molecular weight and solubility, in which the parameters of the solution studied are concentration, viscosity, conductivity and surface tension.

The electrospinning technique is one of the alternative methods of greatest interest in the medical field to fabricate membranes based on intertwined polymeric fibers that allow the encapsulation

of drugs [4] due to their easy absorption. This versatile technique is easy to implement, allowing processes with different polymers. The development of nanotechnology has allowed the control, manipulation, study and fabrication of structures and devices at the nanoscale, and polymeric nanofibers have a significant impact on biomedical sciences by allowing the design and development of new multifunctional artifacts in which it is possible to encapsulate drugs of interest, thus solving some limitations of conventional non-specific drug delivery systems. Encapsulation is a versatile methodology for subsequent drug release because an encapsulated drug has dosing advantages over other delivery forms [4]. Among the most common advantages are decreased lethal side effects, prolonged activity time, and protection for drugs sensitive to enzymatic attack or acid degradation due to local pH.

In this perspective, this research work focuses on fabricating PVAL polymeric nanofibers capable of retaining a drug within its porous matrix of high surface area and thus studying the physical and chemical properties presented by these new materials, as it is a task that can contribute to the development of possible future applications in the field of medicine.

2. MATERIALS AND METHODS.

2.1. Preparation of the polymer solution.

For the polymeric solution, 1 g of PVAL with a molecular weight of 145,000 was dissolved in 15, 16, 18, 19 and 20 ml, respectively, of milli-Q water from MERCK; the process was carried out in a magnetic stirrer, maintaining a temperature of 150°C for 30 minutes, once the polymer was dissolved, the solution was brought to room temperature and left stirring for six (6) hours obtaining a homogeneous polymer/water solution.

2.2. Production of nanofibers by electrospinning technique

The nanofibers were made using the electrospinning technique by injecting the polymeric solution with an infusion pump through an infusion needle that leads to a 21G needle to create a constant drip. A high voltage source connects to the needle and the collector plate to form a potential difference and originate the Taylor cone and thus produce the polymeric fibers; the whole electrospinning system is located inside an acrylic chamber (Fig. 1); for this purpose, several parameters such as relative humidity, temperature, injection flow rate and voltage are experimentally controlled. The effect of the nanofibers was studied by changing the needle-collector distance and the viscosity of the solution.

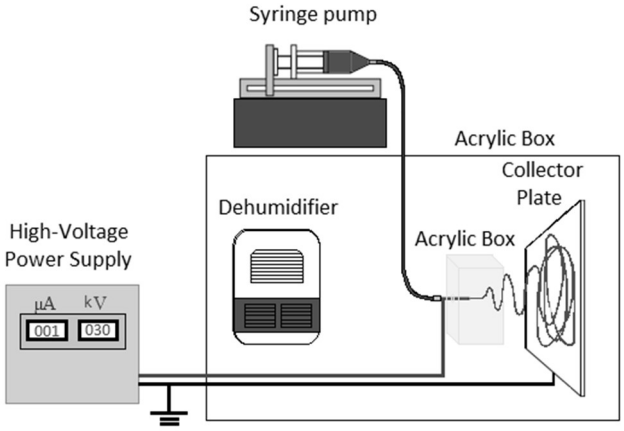

Figure 1. Experimental setup of the electrospinning technique.

2.3. Scanning electron microscopy.

Morphological analysis for the electrospinning fibers was performed using a FEI QUANTA 250 scanning electron microscope (SEM), operating between 5 and 80 kV, a working distance between 8.9 and 10.2 mm and resolutions ranging from 3 to 10 nanometers. The samples were observed with the detectors operating at low vacuum conditions. For each sample, the average fiber diameters were studied at different magnifications and measured using ImageJ software, developed by the National Institutes of Health. Morphological analysis made it possible to determine whether micrometer or nanometer-sized fibers were obtained. Following these criteria, the experimental parameters were modified until nanometer-sized fiber growth was obtained without defects in the form of beads and fractures.

2.4. Fourier transform infrared spectroscopy technique

Subsequently, the nanofibers were characterized based on the molecular level information on functional groups, types of bonds and molecular conformations using the Fourier Transformed Fourier Infrared Spectroscopy (FTIR) technique (4700 JASCO brand). It is important to note that the spectra obtained by the FTIR technique are presented as a function of the wavenumber due to the direct proportionality that exists between this magnitude and the frequency of absorbed radiation that coincides with the frequency of molecular vibration, which is responsible for the absorption process [5].

3. RESULTS AND DISCUSSION.

3.1. Growth and morphological characterization of electrospun nanofibers.

For the growth of the fibers, different parameters were varied, such as applied voltage, distance needle collector, and injection speed, to establish the optimal conditions for obtaining fibers from the prepared solutions. The values of these parameters were experimentally determined in such a way that the loaded polymeric solution, when expelled towards the collector, did not form drops, but a jet or linear jet, which allowed obtaining a very thin white layer on the collector, as an indicator of good growth of the polymeric fibers.

To determine the effect of the needle-collector distance on the fibers, 9, 11, 13 and 15 cm distances were studied to obtain a good fiber morphology, free of surface defects and with a homogeneous diameter distribution. A polymer-water solution with a concentration of 5% (*w/V*) was prepared, an electrical potential difference of 25 kV was applied between the needle and the collector, and a polymer injection rate of 4 µL/h was applied. Inside the fiber growth chamber, a stream of hot, dry air was circulated, being possible to control the relative humidity with a value of 22%, a temperature of 45 ± 0.01 °C and a pressure of 300 ± 0.1 pascals, values that remain constant during the growth time of the polymeric fibers until a membrane of a good thickness was obtained. The control curves of these experimental parameters are shown in Figure 2. The control of these thermodynamic variables of the polymeric fibers' growth allows a high percentage of reproducibility of the samples.

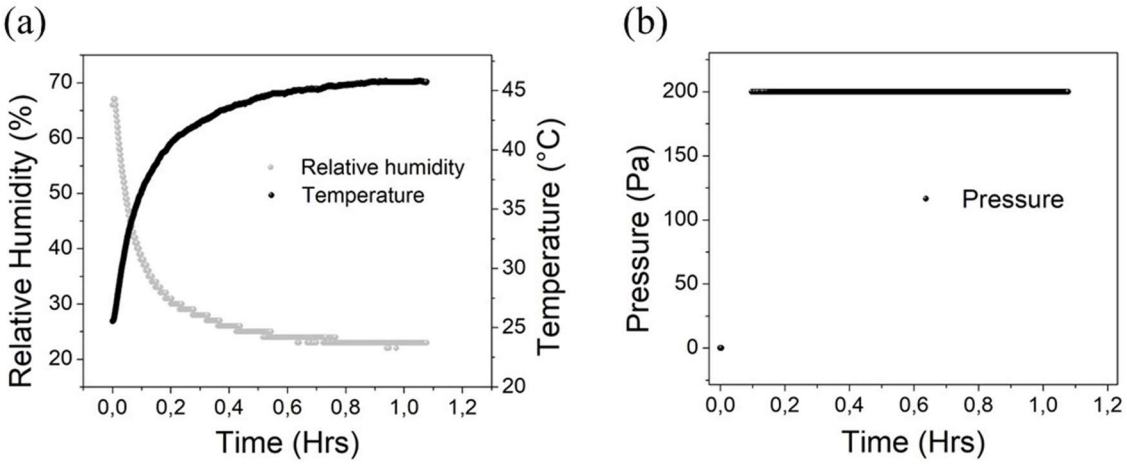

Figure 2. PVAL polymeric fiber growth control curves, a) relative humidity and temperature vs. time, b) pressure vs. time.

The SEM micrographs presented in Figure 3, with optical magnification from right to left of 20,000 and 50,000 X, for the electrospun fibers on aluminum foil substrates and obtained at needle-collector distances of 9, 11, 13 and 15 cm, show imperfections on the surface of the fibers, probably as a consequence of incomplete drying. This is typical of polymer solutions that do not meet the viscosity suitable for electrospinning [6, 7]. All images show an inhomogeneous morphology characterized by structural defects due to the formation of pearls or beads. Fibers grown at a needle-collector distance of 9 and 11 cm (figs.3(a-e)) presented fibers that do not fracture and have fewer beads on their surface. For the samples grown at a needle-collector distance of 13 and 15 cm (figs.3(g-k)), fibers were observed to fracture in relatively short segments of varying diameter due to incomplete spinning. The breakage of the fibers is due to the fact that the drop of the solution, when stretched by the applied electric field, may suffer breakage of the linear jet resulting in broken fibers deposited on the collector plate. There is also a greater presence of beads on their surfaces, increasing the formation of defects as the needle-collector distance increases, so that there is a decrease in the surface area of the nanofibers.

The values of the bead diameters are between 500 and 700 nm, these beads are the result of the formation of droplets in the first stages of the linear jet, which are attributed to the joint action of three types of force, the surface tension that tends to change the jet or linear jet into droplets, electrostatic repulsion between the charges on the jet surface, which does not favor the formation of droplets but rather that of a thin jet, and finally, viscoelastic forces that resist rapid changes in shape and promote the formation of homogeneous fiber surfaces; when the last two interactions cannot counteract the surface tension, bead formation occurs [8, 2].

In the histograms shown on the far right of Figure 3, it can be seen that, for all the samples obtained, the distribution of the average diameter of the fibers when measuring the diameter of 500 fibers is of Gaussian form, the results of which are presented in Table 1, where the values of the average diameter of the fibers, the absolute standard deviation and the percentage standard deviation are observed.

It is observed that the average fiber diameter size is smaller as the distance between the needle and the collector increases, taking values from 137 ± 5 nm to 96 ± 5 nm starting from a needle-collector distance of 9 to 15 cm. These analyses were carried out for 500 fibers of each sample; the percentage standard deviation indicates that as the distance between the needle and the collector increases, the average fiber diameter tends to be more dispersed, indicating that long and smooth fibers with homogeneous diameters are not obtained; however, it can also be observed that at a needle-collector distance of 9 cm, more defects are formed in the form of beads.

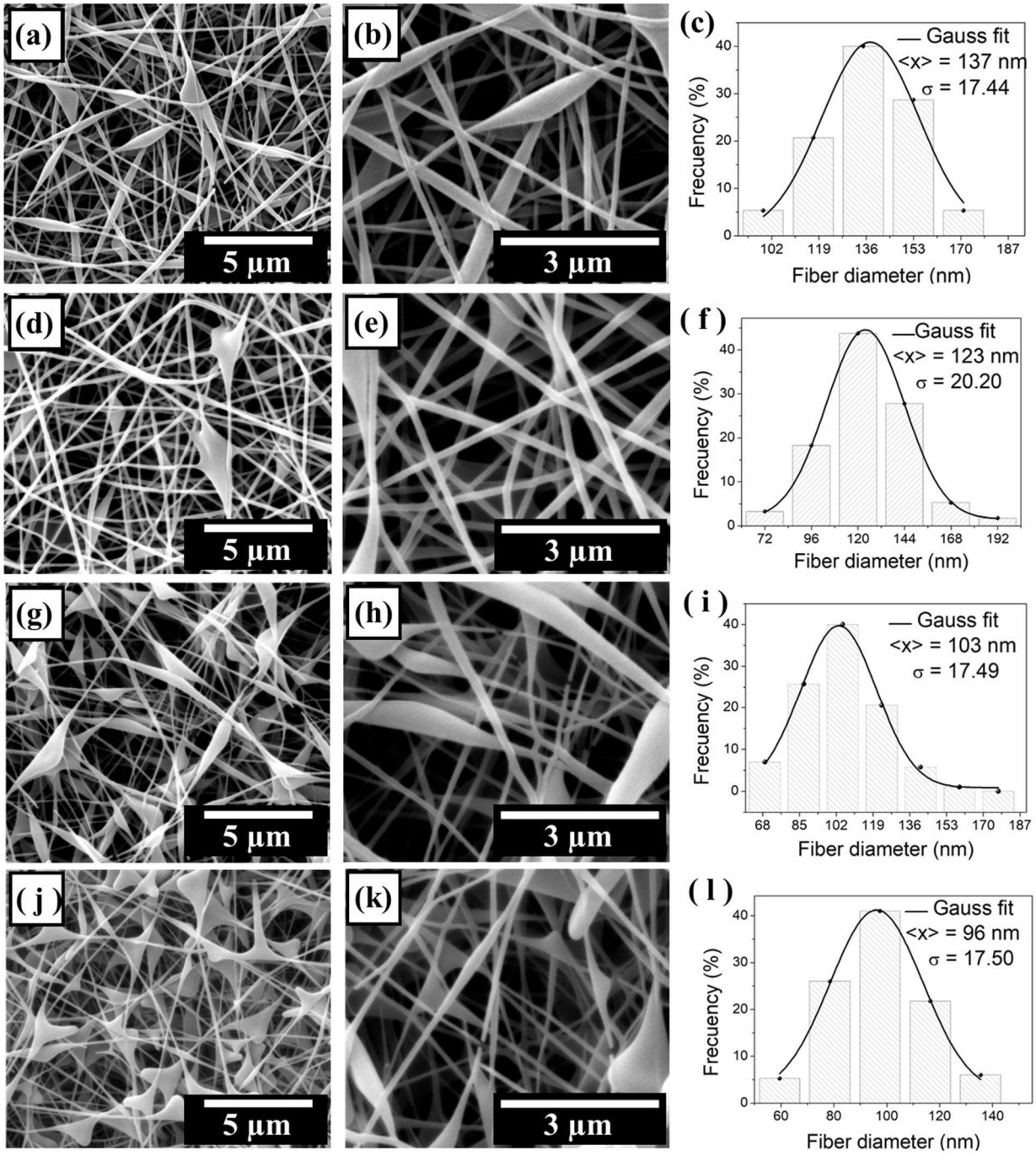

Figure 3. 20,000 and 50,000 X SEM micrographs and diameter distribution histograms for nanofibers grown at a collector needle distance of (a-c) 9 cm, (d-f) 11 cm, (g-i) 13 cm and (g, h) 15 cm.

Table 1. Mean diameter values, absolute standard deviation and percentage standard deviation at different needle-collector distances.

Distance (cm)	Mean diameter (nm)	Standard deviation (nm)	Standard deviation (%)
	137 ± 5	17.44	12.72
	123 ± 5	20.20	16.42
	103 ± 5	17.49	16.98
	96 ± 5	17.50	18.22

The large sections measure 150 ± 5 nm, while the short sections measure 45 nm. The fit to the Gaussian model shown by the diameter distribution is R^2 =0.9882.

In general, the distance from the capillary to the collector is found to influence the size and morphology of the formed nanofibers. It is observed that an increase in the needle-collector distance tends to decrease the diameter of the electrospun nanofibers, as reported by other authors [9, 10].

Once these results were obtained in the first tests, it was sought to improve the properties of the solution so that during the electrospinning process, fibers free of defects were obtained and taking into account that the concentration of the polymer is fundamental to determining the size and morphology of the fibers, it is found that having an optimum viscosity of the solution, it has a positive influence on the electrospinning technique, being able to obtain fibers at a lower voltage than that needed for low viscosities [11]. Therefore, the voltage was lowered to 19 kV, an injection rate of less than 1 µL/h, a needle-collector distance of 11 cm, relative humidity of 30 % using a dehumidifier inside the chamber, a temperature of 30 ± 0.01 ºC and the growth chamber was kept at atmospheric pressure, for 1 hour and 20 minutes to start the growth (Fig.4). The growth time is 2 hours, and a membrane of considerable thickness is obtained, then the characterization is performed with the different techniques. In order to study the effect of such concentrations, four PVA polymeric solutions of 6.66%, 6.25%, 5.55% and 5.26% (*w/V*) mL of milli-Q water were prepared, maintaining the conditions described above.

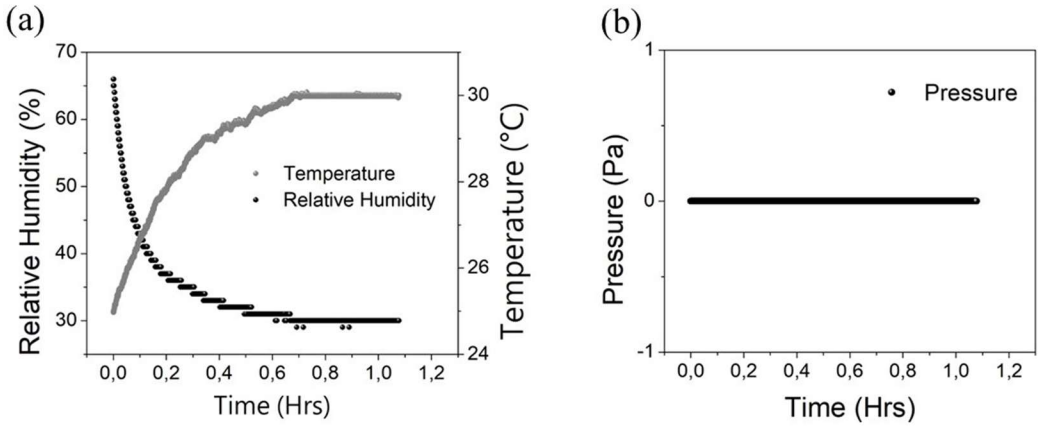

Growth chamber control curves for PVAL polymeric fiber production, a) relative humidity and temperature vs. time, b) pressure vs. time.

The SEM micrographs presented in Figure 5, with optical magnification from left to right of 20,000 and 50,000 X, for electrospun fibers grown at concentrations with a ratio of 6.25%, 5.55% and 5.26% (w/V) show a non-homogeneous morphology due to the presence of bead-shaped defects along the polymeric network. The bead defects generally occur at low concentrations, resulting in the breakage of the polymer into droplets due to the effect of surface tension. Similarly, concentrated solutions do not form fibers due to the high viscosity that hinders the passage of the solution through the capillary [11, 5]

It is observed that the average diameter size of the fibers is larger as the *w/V* ratio increases, as shown in the histograms located on the far right side of Figure 5 (Figs.5(c, f, i)). In the analysis of the histograms shown on the right side of Fig.5, it can be seen that the mean diameter of the fibers ranges from 135 ± 5 nm to 149 ± 5 nm going from a concentration of 5.26% to 6.25%. Furthermore, the standard deviation gives additional information about the homogeneous distribution of the fibers since as the viscosity increases, the standard deviation decreases; therefore, a greater amount of homogeneous fibers can be obtained along the polymeric network. These analyses were performed for 500 fibers of each sample.

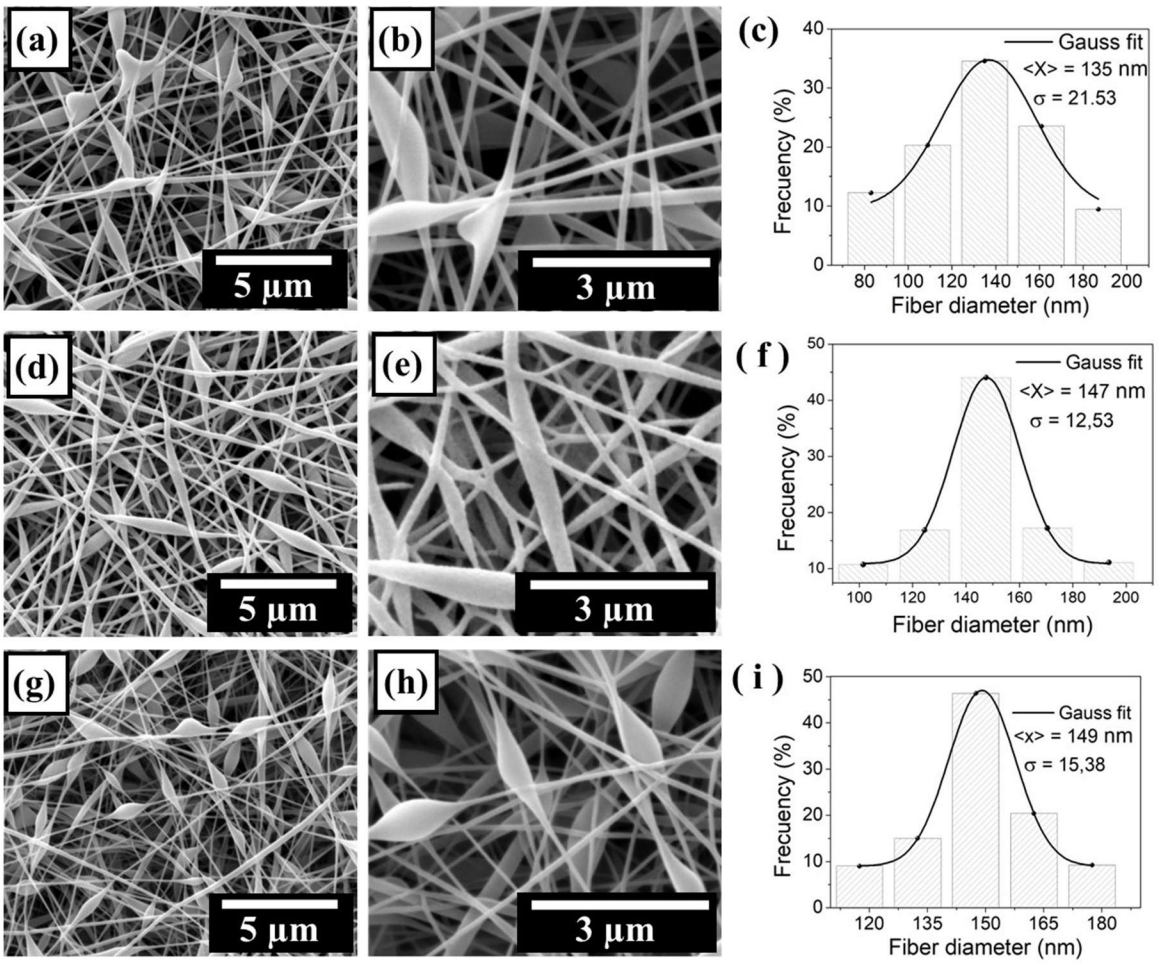

Figure 5. 20,000 and 50,000 SEM micrographs and diameter distribution histograms for nanofibers grown at concentrations (*w/V*) of (a-c) 5.25.25% (d-f) 5.55% and (g-i) 6.25%.

Figure 6 shows micrographs obtained by SEM for PVAL electrospun fibers, at a ratio of 6.66% (w/V), grown under the conditions described above. Images at an optical magnification of 50,000, 20,000 and 10,000 X (Figs.6(a-c)) allow observing much smoother, homogeneous fibers, free of beaded defects and without fractures. Short and long stretches are not observed; they are long and continuous fibers that intertwine with each other randomly, forming a regular morphology. In the analysis of the diameter through the histogram, it can be appreciated that it has a narrow Gaussian diameter distribution, with an average value of 126 ± 5 nm, a standard deviation of 12.63, and a high degree of fit to the Gaussian curve with R^2 =0.9882.

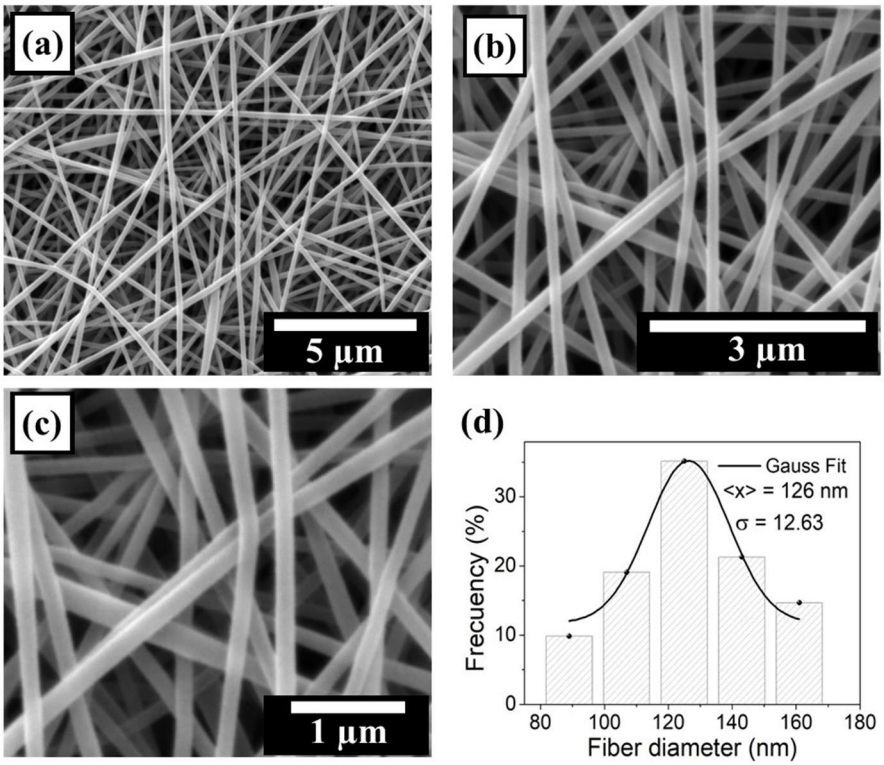

Figure 6. SEM micrographs of PVAL electrospun nanofibers were obtained at 19 kV, an injection rate of 1 µL/h, relative humidity of 30%, a temperature of 30 °C, atmospheric pressure, and collector needle distance of 11 cm. Ratio 6.66% (*w/V*) of PVAL/milli-Q water. Magnification of (a) 50,000 X, (b) 20,000 X and (c) 10,000 X. (d) Histogram of diameter distribution.

The effect suffered by the fibers when changing the needle-collector distance and the viscosity of the polymeric solution is shown in Figure 7. When the needle-collector distance is increased from 9 to 15 cm, there is a decrease in the average diameter of the fibers from 136 ± 5 nm to 96 ± 10 nm. On the other hand, the average diameter of the fibers is greater as the concentration of the solution increases, going from 135 ± 5 nm to 149 ± 5 nm when using polymeric solutions from 5.25% to 6.25%, confirming the effects that Duque and others [12] previously studied.

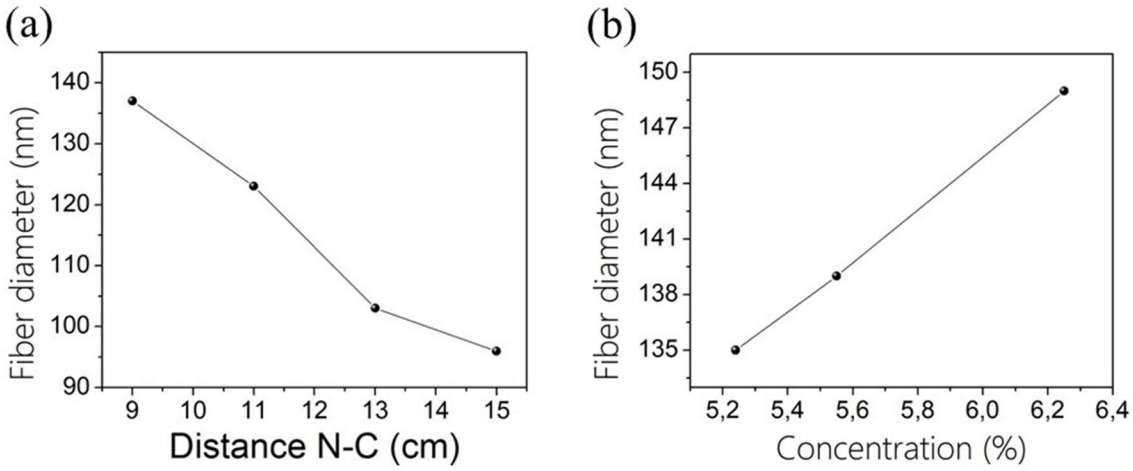

Figure 7. Plots of the effect on the mean fiber diameter as a function of (a) needle-collector distance and (b) solution concentration (W/V).

3.2. Chemical characterization with FTIR

An analysis of infrared absorption spectra performed on a 6.66% (*w/V*) homogeneous PVAL-water milli-Q solution and a solid polymeric membrane of PVAL at the same concentration is presented as a basis for comparison to PVAL electrospun samples.

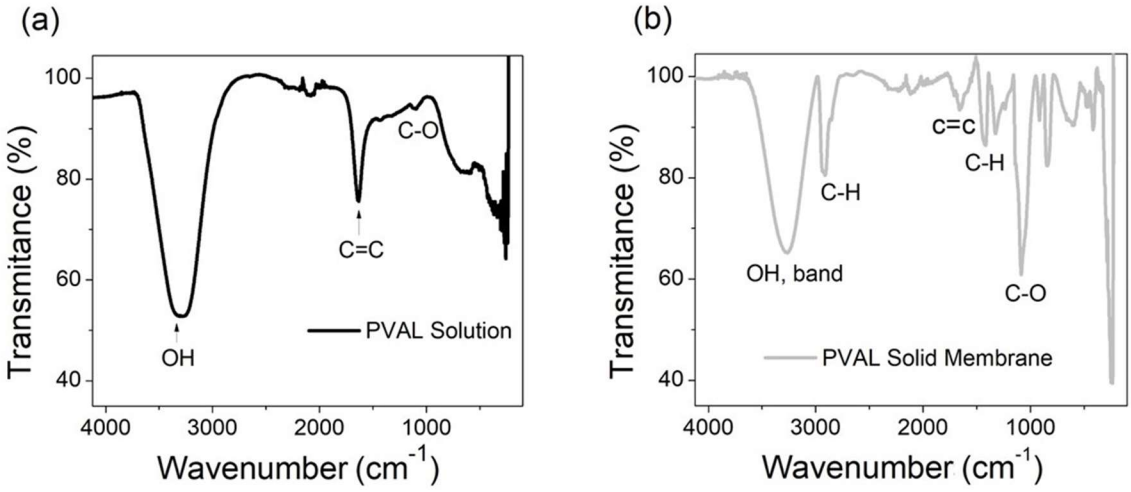

Figure 8. FTIR of PVAL at 6.66% (W/V) in (a) solution and (b) solid membrane.

Figure 8, shows the FT-IR spectrum in absorption mode, performed on a homogeneous solution PVAL-water milli-Q 6.66% (*w/V*) and on a solid film obtained after evaporating the water from the PVAL solution in the range of 400 to 4000 cm^{-1}.

In Fig.8(a), the vibration peak associated with water molecules in the membrane is recorded and centered at 3290.79 cm^{-1}. This is due to the -OH vibration peaks of water deformation [5]; the absorption band at 1096.26 cm^{-1} is due to the stretching modes of the C-C and C-O groups, being

also sensitive to the crystallinity in the polymeric matrix, while the band at 1638.72 cm^{-1} is due to the double bonding of the C=C group.

The vibration peak associated with the hydroxyl group of the polymer side chain is also found at 3264.89 cm^{-1} (Fig.8(b)) due to the absorption band of the oxygen-hydrogen (OH) single bond. The absorption band at 1084.76 cm^{-1} is the deformation mode of the carbon-carbon (C-C) single bond and carbon-oxygen (C-O) single bond groups. The band at 1658.48 cm^{-1} is due to the double bond of the C=C group, a peak corresponding to the C-H stretching at 2912.94 and another at 1416.45 scissor-like vibration due to another C-H bond.

Figure 9(a) shows the FT-IR spectra discussed earlier for the homogeneous solution PVAL-water milli-Q 6.66% (*w/V*) (red curve) and of electrospun PVAL nanofibers (black curve) for comparison. It is found for PVAL nanofibers that the -OH vibrational peak is less broad and runs slightly to the left at 3282.25 cm^{-1}. On the other hand, the absorption band of the stretching modes of the C-O group is a much sharper and more intense peak and runs to the right at 1059.77 cm^{-1}. The above feature may be related to the fact that the polymeric matrices formed by the nanofibers form a more amorphous structure. For the band associated with the double bond of the C=C group, it is found that its peak is much less intense and runs to the left at a value of 1677.13 cm^{-1}. It is hypothesized that the decrease in peak intensity may give evidence that the C=C double bond is broken due to the high potential applied in the electrospinning technique (19 kV).

Furthermore, the appearance of other absorption peaks that do not appear for the homogeneous solution PVAL-water milli-Q at 6.66% (*w/V*) is observed, one around 2925.56 cm^{-1} associated with the (C-H stretching) group, other FTIR absorption peaks at 1309.29 cm^{-1} (C-O stretching), 904.58 cm^{-1} (CH_2 rocking) and 845.42 cm^{-1} (C-C stretching) found by other authors for PVAL [5, 13]. In Figure 9(*b*), the FTIR absorption spectrum of a solid film obtained after evaporating water from the 6.66% (*w/V*) PVAL-water milli-Q solution (blue curve) and the corresponding absorption spectrum of electrospun PVAL nanofibers (black curve) is presented. It is found that the membrane produced by electrospun nanofibers has the same functional groups as the solid PVAL membrane; however, its transmittance peaks are more intense.

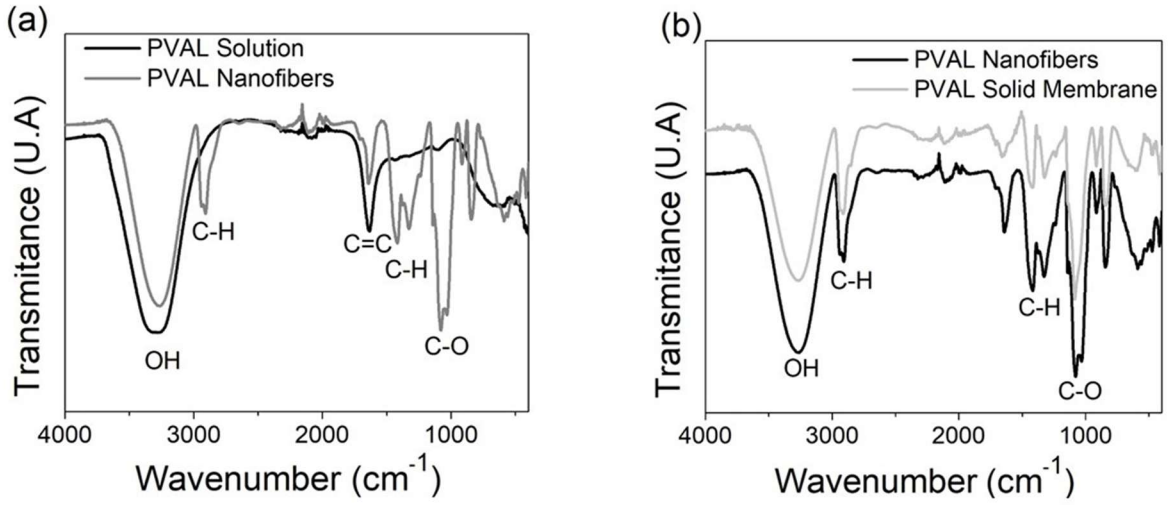

Figure 9. FTIR of PVAL (6.66%) (*w/V*) in (a) solution (black curve) and electrospun nanofibers (gray curve). (b) solid membrane (Lt gray curve) and nanofibers (black curve).

4. CONCLUSIONS

The electrospinning technique becomes an alternative to producing polymeric matrices with an extensive surface area and the possibility of retaining and storing drugs inside them. The effect suffered by the morphology and average diameter of the electrospun fibers was studied by increasing the distance between the needle and the collector between 9 cm and 15 cm, obtaining an average diameter of fibers varying from 136 ± 5 nm to 85 ± 10 nm respectively, a change observed in the morphology of the fibers. Even fibers were found free of pearl-shaped defects for a needle-collector distance of 11 cm. It was also observed that when the polymer solution concentration is increased from 5.26 to 6.25% (*w/V*), the average diameter of the fibers increases from 135 ± 5 nm to 145 ± 5 nm, respectively. However, there is a reduction in the production of bead defects as the percentage concentration increases. An applied voltage of 19 kV, a needle-collector distance of 11 cm, an injection rate of 1 µL / h, a relative humidity of 30%, a temperature of 30 °C, an atmospheric pressure and a solution of 6.66% (*w/V*) were found to be optimal parameters to obtain fibers with a homogeneous diameter and free of defects. The FTIR spectra obtained for the membrane produced with electrospun nanofibers show the same functional groups as the solid PVAL membrane without electrospinning; however, its transmittance peaks are more intense.

References

[1] T. Amna, M. S. Hassan, D. R. Pandeya, M. S. Khil y I. H. Hwang, «Classy non-wovens based on animate L. gasseri-inanimate poly (vinyl alcohol): upstream application in food engineering,» *Applied Microbiology and Biotechnology,* vol. 97, nº 10, pp. 4523-4531, 2013.

[2] E. Franco, s. Delvasto, F. Zuluaga y F. Marti, «Caracterización del haz proyectado en el proceso de electrohilado de PVA.,» *Suplemento de la Revista Latinoamericana de Metalurgia y Materiales,* vol. S1, nº 3, pp. 1097-1103, 2009.

[3] S. Gomez, «Obtención de nanofibras por el método de electrospinning y films biodegradables de amilosa.,» *Instituto Politécnico Nacional. Tesis individual. México.D.F.,* 2013.

[4] M. Lopez Casillas, «Grupo de investigación en la vía L-Arginha Óxido Nítrico,» 2010.

[5] A. M. Shehap, «Thermal and espectroscopy studies of Polyviniyl Alcohol/Sodium Methyl cellulose blends,» *Egypt. J. Solids,* vol. 31, nº 1, pp. 75-91, 2008.

[6] K. F. Fernades, C. S. Lima y C. H. Collins, «Properties of horseradish peroxidase immobilised onto polyaniline,» *Process Biochemistry,* vol. 39, nº 8, pp. 957-962, 2004.

[7] I.-B. Kim y U. Bunz, «Modulating the Sensory Response of a Conjugated Polymer by Proteins: An Agglutination Assay for Mercury Ions in Water,» *Journal of the American Chemical Society,* vol. 128, pp. 2818-2819, 2006.

[8] L. Wu, X. Yuan y J. Sheng, «Immobilization of cellulase in nanofibrous PVA membranes by electrospinning,» *Journal of Membrane Science,* vol. 250, pp. 167-173, 2005.

[9] D. Li y Y. Xia, «Electrospinning of Nanofibers: Reinventing the Wheel,» *Adavanced Materials,* vol. 16, nº 14, pp. 1151-1170, 2004.

[10] G. Taylor, «Electrically Driven Jets,» *Proc R Soc London,* vol. 313, p. 453, 1969.

[11] S. Megelski, J. Stephens y D. Chase, «Micro–and Nanostructured Surface Morphology on Electrospun Polymer Fibers,» *Macromolecules,* vol. 35, p. 8454, 2002.

[12] L. Duque, L. Rodríguez y M. López, «Electrospinning: La era de las nanofibras,» *Revista Iberoamericana de Polímeros,* vol. 14, nº 1, pp. 10-27, 2013.

[13] B. J. Hwang, J. Joseph , Y. Z. Zeng, C. W. Lin y M. Y. Cheng, «Analysis of states of water in poly (vinyl alcohol) based DMFC membranes using FTIR and DSC,» *Journal of Membrane Science,* vol. 369, nº (1-2), pp. 88-95, 2011.